Evolving mortal networks

Jennifer L. Slater, Barry D. Hughes,* and Kerry A. Landman†

Particulate Fluids Processing Centre, Department of Mathematics and Statistics, The University of Melbourne, Victoria 3010, Australia
(Received 8 December 2005; published 8 June 2006)

We discuss a class of models for the evolution of tree networks in which new nodes are recruited into the network at random times, and nodes already in the network may die at random times. Stochastic mechanisms for growth and death of the network that are either sensitive or insensitive to the coordination number or degree of nodes are studied using simulations and mean-field approximations. Critical behavior is observed in the long-time coordination number distribution of the system; associated exponents are universal in one part of parameter space, but depend on the ratio of birth and death parameters elsewhere.

I. INTRODUCTION

Evolving network models have been the focus of many recent studies, discussed in the reviews of Albert and Barábasi [1] and Newman [2] and the monograph of Dorogovtsev and Mendes [3], which also describe important applications of these models. There is particular interest in scale-free networks, which have been used to model networks ranging from the biological (gene-regulatory and metabolic networks) to the social (scientific citation indices) to information networks such as the World Wide Web [4]. Evolving network models have also been applied to the study of processes taking place on networks, such as epidemic spread [5].

Important work in the context of random recursive trees by Szymánski [6,7] that has been little cited to date gave exact results on the discrete-time generation of random trees either with unbiased attachment of new nodes to randomly selected nodes, or with preferential attachment in proportion to the coordination numbers or degrees of the nodes. The latter case, which exhibits a power-law tail in the coordination number distribution [8], is equivalent to the preferential attachment model more recently proposed by Albert and Barábasi [1,4]. Preferential attachment has the effect of accelerating the network growth [3].

Chan *et al.* [9] studied algorithms for generating randomly growing networks in continuous time, producing both trees and cross-linked networks. In their work on trees, two possibilities were considered: a linear birth process, in which every node randomly gives birth to new nodes linked to it at an average rate λ, and a preferential birth process, in which each node randomly gives birth at a rate proportional to its current coordination number. These two cases implement in continuous-time the discrete-time processes of Szymánski. We extend the work of Chan *et al.* [9] to allow for the more realistic scenario where nodes may eventually die.

Previous studies of the role of death in networks have included the notions of random and preferential attack, whereby a certain number of nodes, either chosen at random

or by their high degree, are simultaneously and instantaneously removed from the network [3] and also the notion of decaying networks, where random links are removed as new nodes are added [11]. This is in contrast to the present work, where individual nodes may die independently, at random times. Amaral *et al.* [12] consider the random "inactivation" of links through simulation, while Cooper *et al.* [13] consider the random deletion of nodes and links in an evolving network.

In this paper, both constant and preferential death rates are considered for trees that grow either via linear birth processes or via coordination-number based preferential reproduction. Critical behavior arising from the competition between birth and death is found, as one would reasonably expect, but there is an interesting transition between universal critical exponents and critical exponents that vary continuously with the parameters that set the rates of birth and death.

In Sec. II, we describe the models and the simulation techniques used. Mean-field techniques are used in Sec. III and the results are compared with simulations. The distribution of distances of nodes from the primal node and the distribution of distances between nodes are discussed in Sec. IV. Critical phenomena observed and corresponding exponents are discussed in Sec. V. For clarity, detailed calculations are relegated to the Appendix.

II. THE MODEL

We consider the following model of growing trees, allowing the possibility of death, which generalizes the model described by Chan *et al.* [9]. Suppose that there is a network of n_0 nodes, each of which may be in either of two states, living or dead. We introduce a new node by attaching it to an existing living node. This is analogous to that node having given birth. As well as giving birth, living nodes may die, while dead nodes can undergo no further events. Rather than having the birth and death events governed by stochastic laws associated with the global network structure, we consider purely local events. Each living node experiences its next event, birth or death, independently of other nodes. In each model considered, for a given node at time t, the probability of a specified event (birth or death) occurring

─────────

*Electronic address: b.hughes@ms.unimelb.edu.au

†Electronic address: k.landman@ms.unimelb.edu.au

in the time interval $(t,t+h]$ has the form $\rho h + o(h)$. Standard arguments show that the time of occurrence of the event is exponentially distributed with rate ρ. Birth and death events are associated with distinct rates, and these rates may depend on the current coordination number of the node under consideration.

In the case of constant birth rate, assume that the probability of a living node giving birth in the time interval $(t,t+h]$ is $\lambda h + o(h)$ as $h \to 0$. For the preferential birth model, a node i, with coordination number or degree k_i at time t, gives birth to a new node in the interval $(t,t+h]$ with probability $\lambda k_i h + o(h)$. We consider also both constant and preferential death rates, that is, probabilities of $\mu h + o(h)$ and $\mu k_i h + o(h)$, respectively, that a living node i will die in the interval $(t,t+h]$. Allowing all combinations of constant and preferential birth and death rates, we have four cases [10]:

Case 1: constant birth rate λ, constant death rate μ;
Case 2: variable birth rate λk, constant death rate μ;
Case 3: variable birth rate λk, variable death rate μk;
Case 4: constant birth rate λ, variable death rate μk.

It is possible to scale the system so that only a single parameter, the ratio of birth and death rates, is present. However, this scaling is not adopted here, as it makes the recovery of limiting cases less convenient, and makes the competition between birth and death rates less evident. It is easy to anticipate that in cases 1 and 3, the system is certain to die out if $\lambda < \mu$, but has a nonzero probability of growing forever if $\lambda > \mu$, so that in these cases $\lambda = \mu$ corresponds to a critical point [16]. For case 2, from previous studies corresponding to $\mu = 0$ [9] the effect of the coordination-number dependent birth rate is to produce an overall birth rate 2λ for the system as a whole, so that we anticipate a critical point at $2\lambda = \mu$. The location of the critical point for case 4 is less obvious.

All four cases are amenable to simulation. A tree structure is defined. Each node is numbered, and the number of its mother, the time at which it is born, its number of daughters and the time at which it dies are recorded. Each node is assigned an individual life clock, which is started at its birth time and runs until the node dies, or until the final time set for the simulation is reached. Nodes die independently. Lifetimes are exponentially distributed, with rates μ (cases 1 and 2) or μk (cases 3 and 4), where k is the current coordination number. Each node also carries a reproductive clock, which determines the time when it next produces a single offspring. Times between production of successive offspring from the same mother node are independent, as are the reproduction times for distinct nodes, and these times are exponentially distributed with rates λ or λk, as appropriate. As the simulation proceeds, time is advanced to the time of occurrence of the next scheduled event. In cases of coordination-number dependent rates, the rate in the exponential distribution is changed appropriately after reproduction. Numbers of living and dead nodes, relative frequencies of coordination numbers and other properties of interest are captured as the simulation proceeds.

Results of these simulations are used to gauge the accuracy of analytically determined mean-field approximations to the coordination number distributions of trees in the different cases derived in Sec. III. We note that the methods used by Chan *et al.* [9] to derive exact results for models without death yield some exact results for case 1, including as special cases known results for linear birth and death processes [14,15]. However, the absence of rules relating the sum over coordination numbers of all nodes present to other observables impedes extension of the methods to the more novel cases (cases 2, 3, and 4), so we shall not report any exact results here.

III. MEAN-FIELD THEORY

Let $n(k,t)$ and $m(k,t)$, respectively, denote the number of living nodes with coordination number k at time t, and the number of dead nodes with coordination number k at time t. Neglecting stochastic fluctuations, it is possible to make a deterministic approximation for the system in terms of differential-difference equations.

For all four cases we use the generating functions

$$M(\kappa,t) = \sum_{k=0}^{\infty} m(k,t)\kappa^k, \quad N(\kappa,t) = \sum_{k=0}^{\infty} n(k,t)\kappa^k, \quad (1)$$

to convert differential-difference equations to partial differential equations. For the three cases in which either the birth or the death rate is variable, we start the system with a pair of nodes joined to each other, so that the birth and death mechanisms can both operate immediately. For the constant birth and death rate case, we start with a single node. Thus our initial conditions are

$$m(k,0) = 0, \quad n(k,0) = \begin{cases} \delta_{k,0}, & \text{Case 1,} \\ 2\delta_{k,1}, & \text{Cases 2,3,4,} \end{cases} \quad (2)$$

with corresponding initial conditions

$$M(\kappa,0) = 0, \quad N(\kappa,0) = \begin{cases} 1, & \text{Case 1,} \\ 2\kappa, & \text{Cases 2,3,4,} \end{cases} \quad (3)$$

for the generating functions. Partial differential equations for generating functions can be solved by the method of characteristics or Laplace transform techniques, and for the latter we write

$$\widetilde{N}(\kappa,s) = \int_0^{\infty} e^{-st} N(\kappa,t) dt, \quad (4)$$

with $\widetilde{M}(\kappa,s)$ defined similarly. In cases 3 and 4, where closed-form solutions of the mean-field equations have not been obtained, we deduce the long-time behavior of the system from the location of the rightmost pole in the complex s plane for the inversion integral

$$N(\kappa,t) = \frac{1}{2\pi i} \int_{c-i\infty}^{c+i\infty} e^{st} \widetilde{N}(\kappa,s) ds. \quad (5)$$

Detailed calculations are given in the Appendix. For brevity, let $\Pr\{K(t)=k|\text{live}\}$, $\Pr\{K(t)=k|\text{dead}\}$, respectively, denote the probability that a randomly chosen live or dead node has coordination number k at time t, while $\Pr\{K(t)=k\}$ refers to a

randomly chosen node, which may be dead or alive. The mean-field results for this birth and death process apply also when $\mu=0$, a birth process, and when $\lambda=0$, a death process—provided they relate to quantities that it is sensible to consider in these cases. If $\lambda=0$ and $\mu \neq 0$, then in the limit $t \rightarrow \infty$ all nodes will have died. Therefore, we consider only limiting results for the number of dead nodes, and the proportion of dead nodes (or all nodes) with coordination number k, where $\lambda < \mu$. Similarly, if $\mu=0$ and $\lambda \neq 0$, there will be no dead nodes, so we consider only results pertaining to living nodes, and to all nodes when $\lambda > \mu$. We do not consider the entirely trivial case in which $\lambda=\mu=0$ and the network remains in its initial state forever.

A. Case 1 (λ, μ)

For the case of constant birth rate λ and constant death rate μ, we have

$$\frac{d}{dt}n(k,t) = \lambda n(k-1,t) - \lambda n(k,t) - \mu n(k,t) + \lambda \delta_{k,1} \sum_{j=0}^{\infty} n(j,t),$$
$$(6)$$

$$\frac{d}{dt}m(k,t) = \mu n(k,t).$$
$$(7)$$

Using generating functions and the method of characteristics, we find that $n(0,t)=e^{-(\lambda+\mu)t}$, while for $k \geq 1$,

$$n(k,t) = e^{(\lambda-\mu)t}2^{-k} + e^{-(\lambda+\mu)t}\left(\frac{(\lambda t)^k}{k!} - \sum_{i=1}^{k} 2^{-i}\frac{(\lambda t)^{k-i}}{(k-i)!}\right). \quad (8)$$

The total number of nodes present at time t is

$$n_t = \sum_{k=0}^{\infty} n(k,t) = e^{(\lambda-\mu)t}.$$
$$(9)$$

In the long time limit, the average proportion of living nodes with coordination number $k \geq 1$ is

$$\lim_{t \rightarrow \infty} \Pr\{K(t)=k|\text{live}\} = \lim_{t \rightarrow \infty} \frac{n(k,t)}{n_t} = 2^{-k}, \quad (10)$$

provided $\lambda > 0$. Half of all live nodes have coordination number 1. This predicted distribution for live nodes is the same as that found by Chan *et al.* [9] in the $\mu=0$ case, both rigorously and by mean-field arguments. If $\lambda < \mu$, we expect the tree to die out eventually, so that the conditional distribution found for $\Pr\{K(t)=k|\text{live}\}$ as $t \rightarrow \infty$ applies to a rapidly shrinking fraction of all nodes in those rare trees that are long-lived.

We turn to the coordination number distribution of dead nodes. We find that

$$m(0,t) = \frac{\mu}{\lambda+\mu}(1 - e^{-(\lambda+\mu)t}). \quad (11)$$

For $k \geq 1$ the exact expression for $m(k,t)$, though elementary, is untidy and we exhibit here only the $t \rightarrow \infty$ asymptotic forms for $k \geq 1$. For $\lambda=\mu$, we have $m(k,t) \sim 2^{-k}\lambda t$, while for $\lambda \neq \mu$ we have

$$m(k,t) = \frac{\mu e^{(\lambda-\mu)t}}{(\lambda-\mu)2^k} + \frac{2\mu^2}{(\lambda+\mu)(\mu-\lambda)}\left(\frac{\lambda}{\lambda+\mu}\right)^k$$
$$+ O(t^k e^{-(\lambda+\mu)t}). \quad (12)$$

We remark that although the first term in this equation diverges as $\lambda-\mu \rightarrow 0$ there is an additional contribution hidden in the $O(t^k e^{-(\lambda+\mu)t})$ terms that cancels this divergence. The first term in Eq. (12) dominates the large t behavior for $\lambda > \mu$, while the second dominates for $\lambda < \mu$. In the degenerate limit $\lambda=0$, the first term is decaying, and is of no greater importance than the terms in $O(t^k e^{-(\lambda+\mu)t})$, which have not been explicitly exhibited. The mean-field prediction for the total number of dead nodes at any time t is

$$m_t = \sum_{k=1}^{\infty} m(k,t) = \frac{\mu(e^{(\lambda-\mu)t} - 1)}{\lambda-\mu}. \quad (13)$$

From the $t \rightarrow \infty$ limit of $m(k,t)/m_t$ we obtain the mean-field prediction that for $\lambda > \mu$,

$$\lim_{t \rightarrow \infty} \Pr\{K(t)=0|\text{dead}\} = 0, \quad (14)$$

while for $k \geq 1$,

$$\lim_{t \rightarrow \infty} \Pr\{K(t)=k|\text{dead}\} = 2^{-k} \text{ if } \lambda > \mu. \quad (15)$$

For $\lambda < \mu$, we predict that

$$\lim_{t \rightarrow \infty} \Pr\{K(t)=0|\text{dead}\} = (\mu-\lambda)/(\lambda+\mu) \quad (16)$$

and for $k \geq 1$,

$$\lim_{t \rightarrow \infty} \Pr\{K(t)=k|\text{dead}\} = \frac{2\mu}{\lambda+\mu}\left(\frac{\lambda}{\lambda+\mu}\right)^k. \quad (17)$$

By considering $\lim_{t \rightarrow \infty}[n(k,t)+m(k,t)]/(n_t+m_t)$ we predict that for $k \geq 1$,

$$\lim_{t \rightarrow \infty} \Pr\{K(t)=k\} = \begin{cases} 2^{-k}, & \lambda \geq \mu, \\ \dfrac{2\mu}{\lambda+\mu}\left(\dfrac{\lambda}{\lambda+\mu}\right)^k, & \lambda < \mu. \end{cases} \quad (18)$$

We also predict that

$$\lim_{t \rightarrow \infty} \Pr\{K(t)=0\} = \begin{cases} 0, & \lambda \geq \mu, \\ (\mu-\lambda)/(\lambda+\mu), & \lambda < \mu. \end{cases} \quad (19)$$

Thus we predict that the limiting coordination number distribution 2^{-k} ($k \geq 1$), found by Chan *et al.* [9] for the case $\mu=0$, persists for live nodes for all values of μ, and also applies for $\lambda > \mu$ to dead nodes and to all nodes. However, we predict critical behavior, with a critical point or threshold at $\lambda=\mu$. For $\lambda < \mu$, where dead nodes predominate, a new coordination number distribution is predicted, with the asymptotic decay in proportion to 2^{-k} replaced by decay proportional to $[\lambda/(\lambda+\mu)]^k$.

In Fig. 1 we show the results of one simulation of a large tree for $\mu/\lambda=0.7$ (i.e., in the phase $\lambda \geq \mu > 0$). Although the mean-field theory might be expected to be useful only for averages over many trees, we see that the coordination number distribution 2^{-k} predicted by it fits well except at the
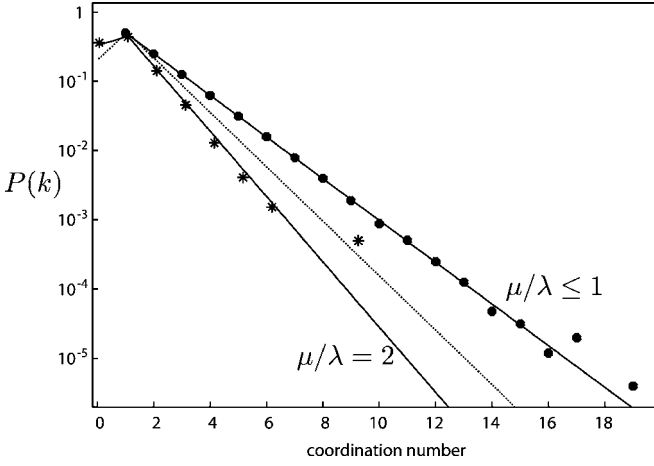
FIG. 1. Case 1 (λ, μ). The mean-field approximation to the long time distribution $P(k)=\lim_{t\to\infty}\Pr\{K(t)=k\}$ for the coordination number of a random node, plotted on a logarithmic scale. The upper solid line corresponds to the mean-field approximation for $0 \leqslant \mu/\lambda \leqslant 1$. The points shown as discs give the coordination number distribution for a single realization of a large tree grown above the threshold ($\mu/\lambda=0.7$ at $\lambda t=40$, giving 251 964 nodes, of which 74 909 were still living). The dotted line and the lower solid line show the mean-field approximation to the distribution for $\mu/\lambda=1.5$ and $\mu/\lambda=2$, respectively. The points shown as asterisks correspond to the averaged coordination number distribution (20) for $r=1000$ realizations at time $\lambda t=40$ with $\mu/\lambda=2$.

largest values of k where there are too few nodes for the statistics to stabilize. For $\mu > \lambda$, since trees are finite with probability 1, the mean-field calculation does not well describe individual realizations of the tree. However, it gives a good prediction of the averaged coordination number distribution

$$\alpha(k) = \frac{\sum\limits_{j=1}^{r} n_j(k,t)}{\sum\limits_{j=1}^{r} n_j(t)} \quad (20)$$

obtained from r realizations of trees, where in the jth realization, there are $n_j(k,t)$ nodes with coordination number k out of $n_j(t)$ nodes generated. Simulation data for $r=1000$, $\lambda t=40$ and $\mu/\lambda=2$ is compared to the mean-field prediction in Fig. 1.

B. Case 2 $(\lambda k, \mu)$

For preferential birth rates but constant death rates,

$$\frac{d}{dt}n(k,t) = \lambda(k-1)n(k-1,t) - \lambda k n(k,t) - \mu n(k,t)$$

$$+ \lambda \delta_{k,1} \sum_{j=0}^{\infty} j n(j,t), \quad (21)$$

$$\frac{d}{dt}m(k,t) = \mu n(k,t). \quad (22)$$

Our chosen initial condition (2) avoids a starting configuration where $k=0$ for all nodes and network growth is impossible. Introducing generating functions and solving by the method of charateristics, we find that

$$n(k,t) = 2e^{(2\lambda-\mu)t} \int_{e^{-\lambda t}}^{1} x^2(1-x)^{k-1}dx + 2e^{-(\lambda+\mu)t}(1-e^{-\lambda t})^{k-1}. \quad (23)$$

We recall for repeated subsequent use in the extraction of large-t asymptotic results that where $k>0$ and $\sigma>0$,

$$\int_{0}^{1} x^{\sigma-1}(1-x)^{k-1}dx = B(\sigma,k) = \frac{\Gamma(\sigma)\Gamma(k)}{\Gamma(\sigma+k)} \sim \frac{\Gamma(\sigma)}{k^{\sigma}} \quad (24)$$

as $k\to\infty$, where we use the standard definitions of the beta and gamma functions. Thus, for example, as $t\to\infty$,

$$n(k,t) \sim \frac{2e^{(2\lambda-\mu)t}\Gamma(3)\Gamma(k)}{\Gamma(k+3)} = \frac{4e^{(2\lambda-\mu)t}}{k(k+1)(k+2)}. \quad (25)$$

Since the total number of live nodes present at time t is predicted to be

$$n_t = \sum_{k=1}^{\infty} n(k,t) = e^{-\mu t}(e^{2\lambda t} + 1), \quad (26)$$

we calculate $\lim_{t\to\infty} n(k,t)/n_t$ and deduce that in mean-field theory,

$$\lim_{t\to\infty} \Pr\{K(t) = k | \text{live}\} = \frac{4}{k(k+1)(k+2)}. \quad (27)$$

Integrating Eq. (22) and recalling that $m(k,0)=0$, we find that for $k \geqslant 1$,

$$m(k,t) = \int_{e^{-\lambda t}}^{1} \frac{2\mu x^2(1-x)^{k-1}(e^{(2\lambda-\mu)t} - x^{\mu/\lambda-2})dx}{2\lambda - \mu}$$

$$+ \int_{e^{-\lambda t}}^{1} \frac{2\mu x^{\mu/\lambda}(1-x)^{k-1}dx}{\lambda}. \quad (28)$$

The second integral in Eq. (28) is

$$\frac{2\mu}{\lambda}B\left(\frac{\mu}{\lambda}+1,k\right) + O\left(\frac{\mu e^{-(\lambda+\mu)t}}{\lambda+\mu}\right),$$

while the first integral adopts different asymptotic forms as $t\to\infty$ depending on the sign of $2\lambda - \mu$,

$$\frac{2\mu e^{(2\lambda-\mu)t}}{(2\lambda-\mu)}B(3,k) \quad \text{if } \lambda > \frac{\mu}{2};$$

$$2\mu t B(3,k) \quad \text{if } \lambda = \frac{\mu}{2};$$

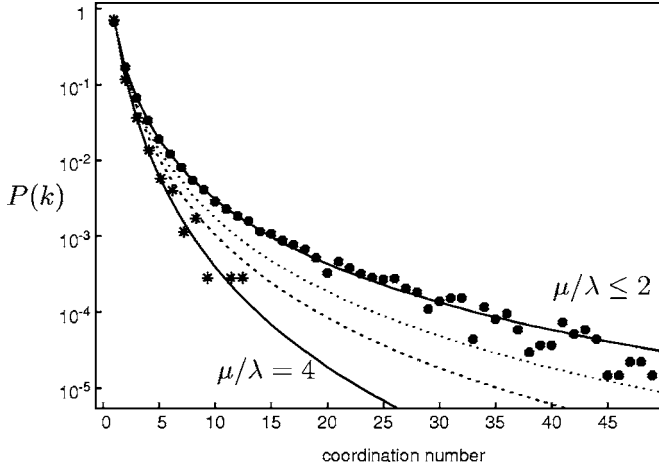FIG. 3. Case 3: $(\lambda k, \mu k)$. Values of the numerically determined parameter s_p plotted as the ratio s_p/λ vs μ/λ.

$\lambda t = 10$, and $\mu/\lambda = 4$ is compared to the mean-field prediction in Fig. 2.

C. Case 3 $(\lambda k, \mu k)$

For preferential birth and death rates, we have

$$\frac{d}{dt}n(k,t) = \lambda(k-1)n(k-1,t) - \lambda k n(k,t) - \mu k n(k,t)$$

$$+ \lambda \delta_{1,k} \sum_{j=0}^{\infty} j n(j,t), \qquad (31)$$

$$\frac{d}{dt}m(k,t) = \mu k n(k,t). \qquad (32)$$

As shown in the Appendix, the Laplace transform of the live-node generating function $N(\kappa,t)$ for $n(k,t)$ is

$$\widetilde{N}(\kappa,s) = \frac{2\widetilde{f}(\kappa,s)}{1 - \lambda \partial \widetilde{f}/\partial \kappa|_{\kappa=1}}, \qquad (33)$$

where, with $_2F_1$ denoting the usual hypergeometric function,

$$\widetilde{f}(\kappa,s) = \frac{\kappa}{s+\lambda+\mu} {}_2F_1\left(1,1;\frac{s}{\lambda+\mu}+2;\frac{\kappa\lambda}{\lambda+\mu}\right).$$

The dominant long time behavior of $N(\kappa,t)$ is determined by the value of s_p, the location of the rightmost pole of $\widetilde{N}(\kappa,s)$. We show in the Appendix that s_p is the unique real solution of the equation

$${}_2F_1\left(1,1;\frac{s_p}{\lambda+\mu}+1;\frac{\lambda}{\lambda+\mu}\right) = 2. \qquad (34)$$

The parameter s_p varies with λ and μ, and is determined numerically (see Fig. 3). It can be proven that $s_p < 0$ when $\lambda < \mu$, that $s_p = 0$ for $\lambda = \mu$, and that

$$s_p/\lambda = 2 - 2(\mu/\lambda)\ln(\lambda/\mu) + O(\mu/\lambda) \text{ as } \mu/\lambda \to 0. \quad (35)$$

For $\mu/\lambda \to \infty$ we have

FIG. 2. Case 2 $(\lambda k, \mu)$. The mean-field approximation to the long time distribution for the coordination number of a random node, $P(k)$, plotted on a logarithmic scale. The upper solid curve corresponds to the mean-field approximation for $0 \leqslant \mu/\lambda \leqslant 2$. The points shown as disks give the coordination number distribution for a single realization of a large tree grown above the threshold ($\mu/\lambda = 0.7$ at $\lambda t = 10$, giving 137 200 nodes, of which 89 541 were still living). The broken curves and the lower solid curve show the mean-field approximation to the distribution for $\mu/\lambda = 2.5$, $\mu/\lambda = 3$, and $\mu/\lambda = 4$, respectively. The points shown as asterisks correspond to the averaged coordination number distribution (20) for $r = 1000$ realizations at time $\lambda t = 40$ with $\mu/\lambda = 4$.

$$\frac{2\mu}{\mu - 2\lambda}B\left(\frac{\mu}{\lambda}+1,k\right) \quad \text{if } \lambda < \frac{\mu}{2}.$$

The total number of dead nodes present at time t is predicted to be

$$m_t = \mu \int_0^t n_\tau d\tau = \frac{\mu(e^{(2\lambda-\mu)t}-1)}{2\lambda-\mu} + 1 - e^{-\mu t} \qquad (29)$$

and from $\lim_{t\to\infty} m(k,t)/m_t$ we deduce that in mean-field theory,

$$\lim_{t\to\infty} \Pr\{K(t) = k | \text{dead}\} = \begin{cases} \dfrac{4}{k(k+1)(k+2)}, & \lambda \geqslant \dfrac{\mu}{2}, \\[2ex] \dfrac{\mu}{\lambda}B\left(\dfrac{\mu}{\lambda}+1,k\right), & \lambda < \dfrac{\mu}{2}. \end{cases} \qquad (30)$$

As in case 1, we predict critical behavior, with a threshold at $\mu/\lambda = 2$. We predict that for $0 \leqslant \mu/\lambda \leqslant 2$, the coordination number distributions for live nodes, for dead nodes, and for all nodes, is the same as that found by Hughes and Reed [15] in the absence of death ($\mu = 0$). This prediction is confirmed for a single realization of a large tree (see Fig. 2). Also as in case 1, in the phase where death has a strong effect ($\mu/\lambda > 2$) the mean-field approximation is not useful for individual realizations of the system, but gives a good estimate of the averaged coordination number distribution $\alpha(k)$ defined by Eq. (20). Simulation data for $r = 1000$,
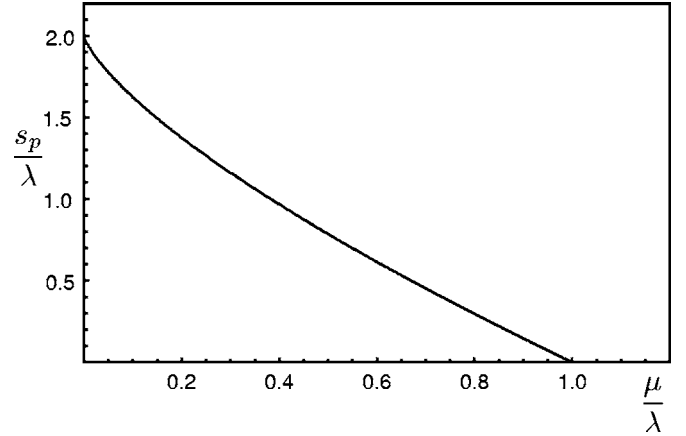
$$\frac{s_p}{\lambda} = -\frac{\mu}{\lambda} + \frac{2\lambda}{\lambda+\mu} + \left(\frac{\lambda}{\lambda+\mu}\right)^2 + O\left(\left(\frac{\lambda}{\lambda+\mu}\right)^3\right). \quad (36)$$

We take the residue at $s=s_p$ of Eq. (33) and expand in terms of the generating function variable, κ. Then,

$$\lim_{t\to\infty} \Pr\{K(t)=k|\text{live}\} = \frac{s_p}{\lambda-\mu}\left(\frac{\lambda}{\lambda+\mu}\right)^k B\left(\frac{s_p}{\lambda+\mu}+1,k\right).$$
$$(37)$$

The number of living nodes is $n_t \sim \text{const} \times e^{s_p t}$. Therefore, the tree is certain to die out if $\lambda < \mu$. Also, when $\mu=0$, we recover the same distribution (27) for $\Pr\{K(t)=k|\text{live}\}$ as was found in case 2 $(\lambda k, \mu)$.

As for the coordination number distribution of dead nodes, we have

$$\widetilde{M}(\kappa,s) = \frac{\mu}{s}\left(\frac{2}{1-\lambda\partial\widetilde{f}/\partial\kappa|_{\kappa=1}}\right)\kappa\frac{\partial\widetilde{f}}{\partial\kappa}(\kappa,s). \quad (38)$$

This has the same singularities as $\widetilde{N}(\kappa,s)$ and an additional singularity at $s=0$. Therefore, when taking the inverse Laplace transform, the dominant behavior of $M(\kappa,t)$ as $t\to\infty$ is determined from the residue at $s=s_p$ when $s_p>0$, and at $s=0$ when $s_p<0$. When $s_p=0$ we have a double pole at $s=0$. This movement of poles is reflected in critical behavior for the coordination number distribution for dead nodes. We have

$$\lim_{t\to\infty} \Pr\{K(t)=k|\text{dead}\}$$

$$= \begin{cases} kB\left(\frac{s_p}{\lambda+\mu}+1,k\right)\left(\frac{\lambda}{\lambda+\mu}\right)^k, & \lambda>\mu, \\ \frac{\mu}{\lambda}\left(\frac{\lambda}{\lambda+\mu}\right)^k, & \lambda\leq\mu. \end{cases} \quad (39)$$

Now, we can show that the fraction of living nodes in the long time limit is $1-\mu/\lambda$, if $\lambda\geq\mu$ and 0 otherwise. By taking a weighted average of Eqs. (37) and (39), we see that

$$\lim_{t\to\infty} \Pr\{K(t)=k\}$$

$$= \begin{cases} \frac{s_p+k\mu}{\lambda}B\left(\frac{s_p}{\lambda+\mu}+1,k\right)\left(\frac{\lambda}{\lambda+\mu}\right)^k, & \lambda>\mu, \\ \frac{\mu}{\lambda}\left(\frac{\lambda}{\lambda+\mu}\right)^k, & \lambda\leq\mu. \end{cases}$$
$$(40)$$

Similarly to case 1 (λ,μ) and case 2 $(\lambda k, \mu)$, we see a threshold, on one side of which trees may grow indefinitely. On the other side, the tree is certain to die out. In this case, the threshold occurs when $\lambda=\mu$, reflecting the balance between preferential birth and preferential death processes. The same threshold was seen in case 1 (λ,μ), when the birth and death processes were both constant. Unlike the earlier two cases, where the coordination number distribution was independent of μ for values of μ in the phase where trees may grow forever, we now see a coordination number distribution
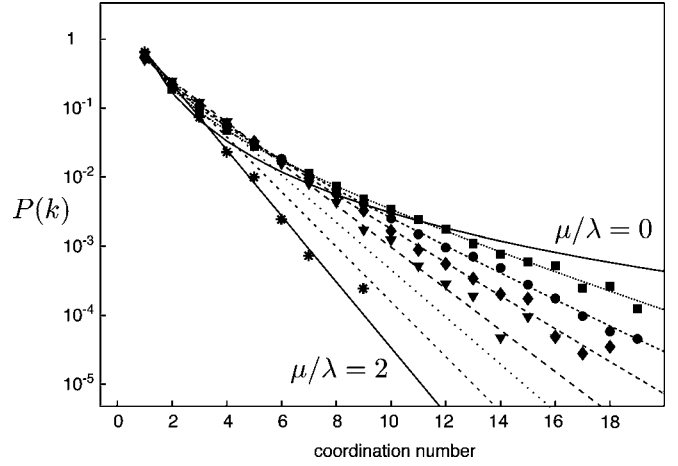

FIG. 4. Case 3 $(\lambda k, \mu k)$. The mean-field approximation to the long time distribution $P(k)$ for the coordination number of a random node; $P(k)$ is plotted on a logarithmic scale. The upper solid curve is the mean-field approximation for $\mu=0$. The mean-field approximations for $\mu/\lambda=0.3$, 0.5, 0.7, 1.0 are the upper four broken curves, with corresponding simulation results for large trees shown as squares, disks, diamonds, and triangles respectively. The simulated trees had 193 508, 153 768, 143 226, 21 039 nodes, with 135 258, 76 874, 43 301, 178 living nodes, respectively, at times from $\lambda t=5.0$ to $\lambda t=40.0$. The lower two broken curves and the lower solid curve show the mean-field approximation for cases where the tree is certain to die out, where $\mu/\lambda=1.2$, 1.5, and 2, respectively. The points shown as asterisks correspond to the averaged coordination number distribution (20) for $r=1000$ realizations at time $\lambda t=10$ with $\mu/\lambda=2$.

which varies with μ everywhere. This may be an effect introduced by the preferential death process. The distribution shows algebraically modulated exponential decay for large k in the phase where trees may grow forever, and exponential decay in the phase where death dominates. The mean-field theory predictions are compared to simulations in Fig. 4.

D. Case 4 $(\lambda, \mu k)$

For the final case, we consider the combination of a constant birth rate and preferential death rate. We have

$$\frac{d}{dt}n(k,t) = \lambda n(k-1,t) - \lambda n(k,t) - \mu k n(k,t) + \lambda\delta_{1,k}\sum_{j=0}^{\infty}n(j,t),$$
$$(41)$$

$$\frac{d}{dt}m(k,t) = \mu k n(k,t). \quad (42)$$

The analysis is very similar to case 3 $(\lambda k, \mu k)$. As discussed in the Appendix, we find that the Laplace transform of the generating function $N(k,t)$ is given by

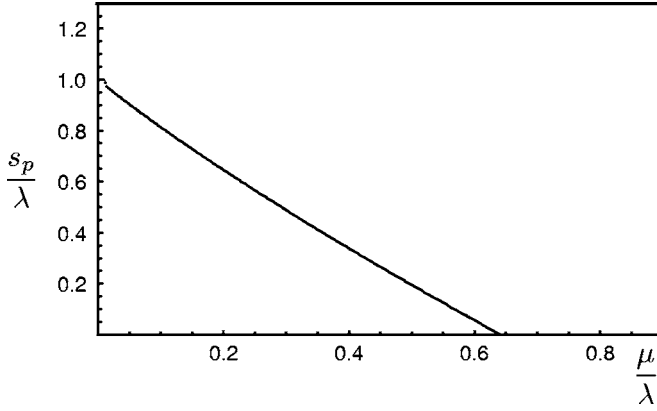$$\widetilde{N}(\kappa,s) = \frac{2\widetilde{f}(\kappa,s)}{1-\lambda\widetilde{f}(1,s)}, \quad (43)$$

where

FIG. 5. Case 4 $(\lambda, \mu k)$. Values of s_p/λ vs μ/λ. Note that $s_p = 0$ when $\lambda = c\mu$, where $c \simeq 1.556$, corresponding to $\mu/\lambda \simeq 0.6427$.

$$\widetilde{f}(\kappa, s) = \frac{\kappa}{\lambda + \mu + s} \, {}_1F_1\left(1; \frac{\lambda + 2\mu + s}{\mu}; \frac{\lambda\kappa}{\mu}\right), \quad (44)$$

where ${}_1F_1$ is the usual confluent hypergeometric function. The only singularity of $\widetilde{N}(\kappa, s)$ is a pole at $s = s_p$, where s_p is the solution (computed numerically, see Fig. 5) of

$$ {}_1F_1(1; (\lambda + \mu + s_p)/\mu; \lambda/\mu) = 2. \quad (45)$$

We also have the asymptotic expansions

$$s_p/\lambda = -\mu/\lambda + \lambda/\mu - \frac{1}{2}(\lambda/\mu)^2 + O((\lambda/\mu)^3) \quad (46)$$

as $\mu/\lambda \to \infty$ and

$$s_p/\lambda = 1 - 2\mu/\lambda + 2(\mu/\lambda)^2 + O((\mu/\lambda)^3) \quad (47)$$

as $\mu/\lambda \to 0$.

Taking the residue at $s = s_p$ of Eq. (43) and expanding in terms of the generating function variable gives

$$\lim_{t \to \infty} \Pr\{K(t) = k | \text{live}\} = \frac{(\lambda/\mu)^k}{(\lambda/\mu + 1 + s_p/\mu)_k}, \quad (48)$$

where $(\alpha)_k = \Gamma(k + \alpha)/\Gamma(\alpha)$. Again, the number of living nodes is $n_t \sim \text{const} \times e^{s_p t}$. Therefore, when $s_p < 0$, the tree is certain to die out eventually. In this case, the threshold occurs at $\lambda = c\mu$, where a numerical solution gives $c \simeq 1.556$ (corresponding to $\mu/\lambda \simeq 0.6427$) [17]. Note that as $\mu \to 0$, we recover the distribution $\lim_{t \to \infty} \Pr\{K(t) = k | \text{live}\} = 2^{-k}$, which was found in case 1 (λ, μ).

The coordination number distribution of dead nodes is found from

$$\int_0^\infty e^{-st} M(\kappa, t) dt = \frac{2\mu\kappa}{s(1 - \lambda\widetilde{f}(1, s))} \frac{\partial\widetilde{f}}{\partial\kappa}(\kappa, s). \quad (49)$$

As in case 3 $(\lambda k, \mu k)$, this has the same singularity structure as $\int_0^\infty e^{-st} N(\kappa, t) dt$, plus an additional singularity when $s = 0$. Therefore, when taking the inverse Laplace transform, the dominant behavior of $M(\kappa, t)$ as $t \to \infty$ is determined from the residue at the rightmost pole, that is, at $s = s_p$ when

$\lambda > c\mu$, at $s = 0$ when $\lambda < c\mu$, and at the double pole $s = 0$ when $\lambda = c\mu$. Therefore, the coordination number distribution for dead nodes exhibits a threshold at $\lambda = c\mu$. We have

$$\lim_{t \to \infty} \Pr\{K(t) = k | \text{dead}\}$$

$$= \begin{cases} \dfrac{(\lambda/\mu)^k}{(\lambda/\mu + s_p/\mu + 1)_k} \dfrac{k\mu}{\lambda - s_p}, & \lambda > c\mu, \\[4mm] \dfrac{k(\lambda/\mu)^{k-1}}{(\lambda/\mu + 1)_k}, & \lambda < c\mu. \end{cases} \quad (50)$$

It can be shown that the fraction of nodes living after a long time is s_p/λ. By taking a weighted average of the distributions for living and dead nodes, we see that the coordination number distribution for all nodes is

$$\lim_{t \to \infty} \Pr\{K(t) = k\}$$

$$= \begin{cases} \dfrac{(\lambda/\mu)^k}{(\lambda/\mu + s_p/\mu + 1)_k} \dfrac{s_p + k\mu}{\lambda}, & \lambda > c\mu, \\[4mm] \dfrac{k(\lambda/\mu)^{k-1}}{(\lambda/\mu + 1)_k}, & \lambda < c\mu. \end{cases} \quad (51)$$

As in case 3 $(\lambda k, \mu k)$, the coordination number distribution is dependent on μ both above and below the threshold. This appears to be due to the preferential death rate. The distribution displays super exponential decay, reflecting the dominance of the preferential death process over the constant death process (see Fig. 6).

IV. RING NUMBER AND PATH LENGTH

The coordination number distribution is a local characterization of the structure of a random network. For a more global characterization of structure, we briefly consider the distribution of path lengths within the network.

We first consider the distribution of the distance of nodes in the network from the primal node from which the network has grown. (When networks are initiated with two nodes, one of these is designated as the primal node.) Following Chan *et al.* [9] we call the distance from the primal node the "ring number." For a randomly chosen node, the ring number R is a random variable with a probability distribution $\Pr\{R = r\} = \phi_R(r)$. For a network of a prescribed size or at a prescribed time, the distribution $\phi_R(r)$, and its associated mean $\langle R \rangle$ and standard deviation σ_R, depend on the parameter ratio μ/λ and on which of cases 1–4 is being considered. However, when we consider the distribution of the scaled ring number $(R - \langle R \rangle)/\sigma_R$, we find that the simulation data for all four cases, and for a wide range of parameter ratios μ/λ including the extreme case of no death $(\mu = 0)$, is well approximated by a single curve for large times, as shown in Fig. 7. Thus, as a good approximation,

$$\phi_R(r) \approx \sigma_R^{-1} \Phi((R - \langle R \rangle)/\sigma_R), \quad (52)$$

with Φ independent of the case considered and the parameter ratio μ/λ. In particular, this curve coincides with the $t \to \infty$ ring number distribution for the case $\mu = 0$, which is known

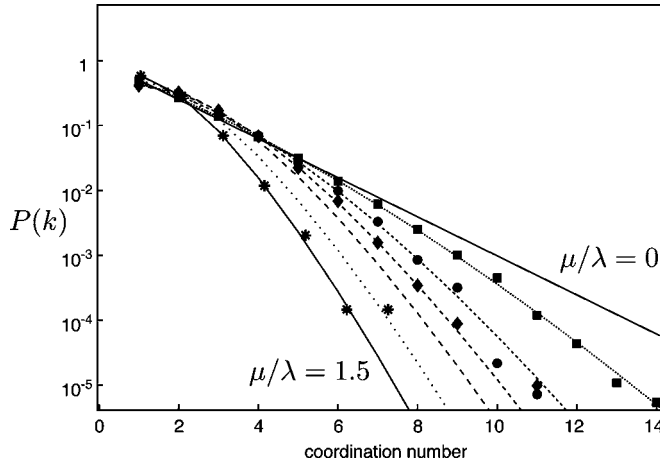FIG. 6. Case 4 $(\lambda, \mu k)$. The mean-field approximation to the long time distribution $P(k)$ for the coordination number of a random node; $P(k)$ is plotted on a logarithmic scale. The upper solid curve is the mean-field approximation for $\mu=0$. The mean-field approximations above the threshold with $\mu/\lambda=0.1$, 0.3, 0.5 are the upper three broken curves, with corresponding simulation results for large trees shown as squares, discs and diamonds respectively. The simulated trees had 185 707, 139 273, 102 526 nodes, with 151 043, 67 799, 19 853 living nodes, respectively, at times from $\lambda t=5.0$ to $\lambda t=40.0$. The lower two broken curves and the lower solid curve show the mean-field approximation to the distribution below the threshold, where $\mu/\lambda=0.7$, 1, and 1.5, respectively. The points shown as asterisks correspond to the averaged coordination number distribution (20) for $r=1000$ realizations at time $\lambda t=10.0$ with $\mu/\lambda=1.5$.

[9] exactly for constant birth rates and in the mean-field approximation for coordination-number dependent birth rates.

The distribution of path length L between a pair of randomly chosen nodes in the network is perhaps the global property of greatest interest in networks. For trees, the shortest path is unique and easily determined by simulation. Where $\langle L \rangle$ and σ_L are the mean and standard deviation of the path length, we find (Fig. 8) that the path length distribution $\Pr\{L=l\}=\phi_L(l)$ is also well-approximated by a scaling form,

$$\phi_L(l) \approx \sigma_L^{-1} \chi((l - \langle L \rangle)/\sigma_L), \qquad (53)$$

with χ independent of the case considered and the parameter ratio μ/λ.

Thus, although network growth rates are heavily influenced by which of the four cases is considered and by the parameter ratio μ/λ, for large networks in the interval of μ/λ that sustains growth, ring number and path length distributions are approximately universal in the sense of Eqs. (52) and (53). Although the distributions found resemble the Gaussian or normal distribution, they are not Gaussian; an explicit, rigorously determined non-Gaussian form for case 1 with $\mu=0$ has been given by Chan *et al.* [9].

V. DISCUSSION

We have considered four models for evolving mortal networks. In each case, a model by which individual nodes give
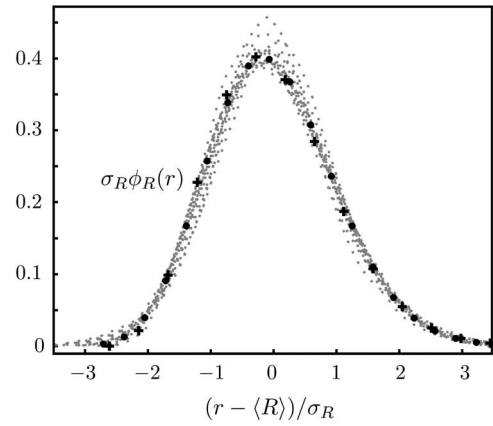

FIG. 7. Scaled ring number distributions $\sigma_R \phi_R(r)$ for all four cases for a variety of death rate to birth rate ratios μ/λ. The gray broken lines indicate average distributions over 100 trees of 10 000 nodes. Data corresponds to $\mu/\lambda=0.1$, 0.3, 0.5, 0.8 for case 1 (λ, μ) and case 3 $(\lambda k, \mu k)$; to $\mu/\lambda=0.1$, 0.3, 0.5, 0.8, 1.0, 1.5 for case 2 $(\lambda k, \mu)$; and to $\mu/\lambda=0.1$, 0.3, 0.5 for case 4 $(\lambda, \mu k)$. The black disks indicate the scaled exact ring number distribution found by Chan *et al.* [9] in case 1 with no death. The black crosses indicate the mean-field ring number distribution found by the same authors for case 2 with no death.

birth to new nodes and/or die was specified, and the resulting network was studied. The limiting coordination number distribution,

$$P(k) = \lim_{t \to \infty} \Pr\{K(t) = k\} \qquad (54)$$

was sought. Mean-field approximations to this distribution were found in all cases and compared to simulation results. Mean-field theory predicts critical behavior as the parameters λ and μ are varied. In each case, there is a critical value of
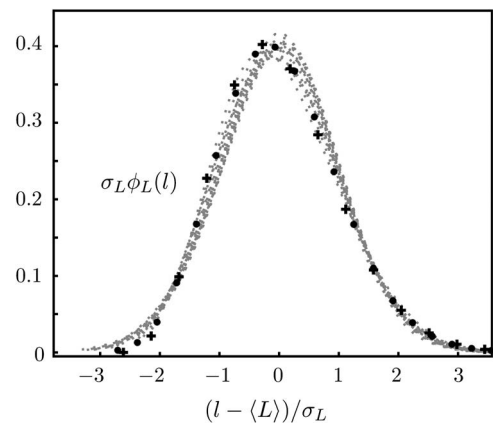

FIG. 8. Scaled path length distributions $\sigma_L \phi_L(l)$ for all four cases for a variety of death rate to birth rate ratios μ/λ. The gray broken lines indicate average distributions over 100 trees of 10 000 nodes. Values of μ/λ considered are as in Fig. 7. The black disks indicate the scaled path length distributions in case 1 with no death obtained by Chan *et al.* [9] using mean-field techniques. The black crosses indicate the approximate distribution in case 2 with no death from Chan *et al.* [9].

the ratio μ/λ that divides parameter space into a "birth-dominated phase" (small μ/λ), where trees may grow arbitrarily large (mean size grows exponentially with time), and a "death-dominated phase" (large μ/λ), for which the trees are certain to die eventually. At the threshold or critical value of μ/λ the mean tree size grows algebraically rather than exponentially.

In the first case, where the birth and death rates are constant, the mean-field theory predicts that the coordination number distribution of the tree converges as $t \to \infty$ for $k \geq 1$ to

$$P(k) = \begin{cases} 2^{-k}, & 0 \leq \mu/\lambda \leq 1, \\ 2(\mu/\lambda)(1 + \mu/\lambda)^{-k-1}, & \mu/\lambda > 1. \end{cases} \quad (55)$$

Also, $P(0) = \max\{(\mu - \lambda)/(\mu + \lambda), 0\}$. So there is a threshold in the behavior of the distribution when $\lambda = \mu$. In the birth-dominated phase, $\lambda > \mu$, the coordination number distribution 2^{-k} found by Chan *et al.* [9] for constant birth process with no death is recovered. For the death-dominated phase, $\lambda < \mu$, the coordination number distribution still decays exponentially, but the attrition factor is explicitly dependent on μ/λ.

In the second case, we considered preferential birth and constant death processes. For large k,

$$P(k) \sim \begin{cases} Ck^{-3}, & 0 \leq \mu/\lambda \leq 2, \\ Ck^{-(1 + \mu/\lambda)}, & \mu/\lambda > 2. \end{cases} \quad (56)$$

(Here, and subsequently, C denotes a factor independent of k, whose value is not necessarily the same from line to line.) In this case, the threshold occurs at $\mu/\lambda = 2$, reflecting the fact that a tree generated by a preferential birth process grows as $e^{2\lambda t}$ [9], while a constant death process causes the number of living nodes in a tree to decay as $e^{-\mu t}$. The coordination number distribution with no death found by Chan *et al.* [9] was recovered for $0 \leq \mu/\lambda \leq 2$. Note that in the birth-dominated phase, the exponent of the power law is universally 3, independent of μ, while in the death-dominated phase the exponent becomes $1 + \mu/\lambda$. For all values of λ and μ the coordination number distribution decays algebraically with k.

In the third case, we considered preferential birth and death processes. For large k,

$$P(k) \sim (1 + \mu/\lambda)^{-k} \times \begin{cases} Ck^{-s_p/(\lambda + \mu)}, & 0 \leq \mu/\lambda \leq 1, \\ C, & \mu/\lambda > 1. \end{cases} \quad (57)$$

The parameter s_p is numerically determined; $s_p < 2\lambda$ for $\mu/\lambda < 1$ and $s_p \to 0$ as $\mu/\lambda \to 1$ from below. Here the threshold returns to $\lambda = \mu$, reflecting the balance between the birth and death processes. We see an algebraically modulated exponential distribution, where the algebraic exponent takes the parameter-dependent value $s_p/(\lambda + \mu)$ in the birth-dominated phase and is universally zero in the death-dominated phase, opposite to the behavior seen in the previous case. Also, the exponential factor in the coordination number distribution is dependent on μ/λ both above and below the threshold.

In the fourth case we considered a constant birth process and a preferential death process. For large k,

$$P(k) \sim \left(\frac{\lambda}{\mu}\right)^k e^{-k(\log(k)-1)} \times \begin{cases} Ck^{1/2-(\lambda+s_p)/\mu}, & \lambda > c\mu, \\ Ck^{1/2-\lambda/\mu}, & \lambda < c\mu, \end{cases} \quad (58)$$

where $c \simeq 1.556$ and $s_p < \lambda$ and both are determined numerically. Here, the threshold is at $\lambda \simeq 1.556\mu$ ($\mu/\lambda \simeq 0.6427$). We see superexponential decay, modulated by a power law which now has a variable exponent in both phases, although the form of the exponent is more complicated (through s_p) in the birth-dominated phase.

We have explored the effect of the interplay of mortality and growth on the coordination number distributions seen in tree networks. These prototype investigations could be extended to more subtle structures in which cross linking is introduced [9] to allow for the clustering that is commonly seen in real networks. These extensions are currently being investigated.

APPENDIX: MEAN-FIELD ANALYSIS

1. Case 1 (λ, μ)

Taking the sum over k of Eqs. (6) and (7) gives partial differential equations for $N(\kappa, t)$ and $M(\kappa, t)$,

$$\frac{\partial N}{\partial t} + (\lambda + \mu - \lambda\kappa)N = \lambda\kappa\phi(t), \quad (A1)$$

$$\frac{\partial M}{\partial t} = \mu N, \quad (A2)$$

where $\phi(t) = N(1, t)$, so $\phi(0) = 1$ from the initial condition (3). On setting $\kappa = 1$ in Eq. (A1) we have $\phi'(t) + (\mu - \lambda)\phi(t) = 0$, so that $\phi(t) = e^{(\lambda - \mu)t}$. With $\phi(t)$ now known, Eq. (A1) is solved by introducing the integrating factor $e^{(\lambda + \mu - \lambda\kappa)t}$ and using the initial condition (3), giving

$$N(\kappa, t) = \frac{\kappa}{2 - \kappa}e^{(\lambda - \mu)t} + \frac{2 - 2\kappa}{2 - \kappa}e^{\lambda\kappa t - (\lambda + \mu)t}. \quad (A3)$$

When the right-hand side is expanded in powers of κ, Eq. (8) is obtained. Equation (A2) can now be solved for $M(\kappa, t)$, again using the appropriate initial condition (3), giving

$$M(\kappa, t) = \frac{\mu\kappa(e^{(\lambda-\mu)t} - 1)}{(\lambda - \mu)(2 - \kappa)} + \frac{2\mu(1 - \kappa)(e^{\lambda\kappa t - (\lambda + \mu)t} - 1)}{(\lambda\kappa - \lambda - \mu)(2 - \kappa)}. \quad (A4)$$

Expanding this in powers of κ produces Eq. (12).

2. Case 2 ($\lambda k, \mu k$)

Equations (21) and (22) lead to partial differential equations for the generating functions N and M,

$$\frac{\partial N}{\partial t} + \lambda\kappa(1 - \kappa)N = -\mu N + \lambda\kappa\phi(t), \quad (A5)$$

$$\frac{\partial M}{\partial t} = \mu N, \tag{A6}$$

where

$$\phi(t) = \frac{\partial}{\partial \kappa} N(\kappa, t)\big|_{\kappa=1}. \tag{A7}$$

From the initial conditions (3), we have $\phi(0)=2$. Equation (A5) can be solved using the method of characteristics [18]. The solutions of $d\kappa/dt=\lambda\kappa(1-\kappa)$ are $e^{\lambda t}(1-\kappa)/\kappa=X$, where X is a constant, so that

$$\kappa = \frac{1}{1 + Xe^{-\lambda t}}. \tag{A8}$$

If we let $N(\kappa,t)=\Phi(X,t)$, then

$$\frac{\partial \Phi}{\partial t} + \mu\Phi = \frac{\lambda\phi(t)}{1 + Xe^{-\lambda t}}. \tag{A9}$$

Using the integrating factor $e^{\mu t}$ and the initial condition (3), which corresponds to $\Phi(X,0)=2/(1+X)$, we easily determine $\Phi(X,t)$ and eliminating X in favor of κ we have

$$N(\kappa,t) = \lambda e^{-\mu t} \int_0^t \frac{\kappa e^{\mu\tau}\phi(\tau)d\tau}{\kappa + e^{\lambda(t-\tau)}(1-\kappa)} + 2e^{-\mu t}\frac{\kappa}{\kappa + e^{\lambda t}(1-\kappa)}. \tag{A10}$$

Differentiating Eq. (A10) with respect to κ and evaluating at $\kappa=1$ gives a consistency equation for $\phi(t)$,

$$\phi(t) = \lambda e^{(\lambda-\mu)t} \int_0^t e^{(\mu-\lambda)\tau}\phi(\tau)d\tau + 2e^{(\lambda-\mu)t}. \tag{A11}$$

Let $\phi(t)=e^{(\lambda-\mu)t}\chi(t)$, so

$$\chi(t) = \lambda \int_0^t \chi(\tau)d\tau + 2,$$

giving $\chi'(t)=\lambda\chi(t)$, with $\chi(0)=2$, and so $\chi(t)=2e^{\lambda t}$ and $\phi(t)=2e^{(2\lambda-\mu)t}$. Now Eq. (A10) becomes

$$N(\kappa,t) = 2\lambda\kappa e^{-\mu t} \int_0^t \frac{e^{2\lambda\tau}d\tau}{\kappa + e^{\lambda(t-\tau)}} + \frac{2\kappa e^{-\mu t}}{\kappa + e^{\lambda t}(1-\kappa)},$$

which can be expanded in powers of κ as

$$N(\kappa,t) = 2\lambda e^{\mu t}\sum_{i=1}^{\infty} \int_0^t e^{\lambda(3\tau-t)}(1 - e^{\lambda(\tau-t)})^{i-1}d\tau\kappa^i$$

$$+ 2e^{-(\lambda+\mu)t}\sum_{i=1}^{\infty} (1 - e^{-\lambda t})^{i-1}\kappa^i. \tag{A12}$$

and Eq. (23) follows if we write $x=e^{-\lambda(t-\tau)}$.

3. Case 3 ($\lambda k, \mu k$)

From Eqs. (31) and (32) the partial differential equations for the generating functions $N(\kappa,t)$ and $M(\kappa,t)$ are

$$\frac{\partial N}{\partial t} + \kappa(\lambda + \mu - \lambda\kappa)\frac{\partial N}{\partial \kappa} = \lambda\kappa\phi(t), \tag{A13}$$

$$\frac{\partial M}{\partial t} = \mu\kappa\frac{\partial N}{\partial \kappa}, \tag{A14}$$

where

$$\phi(t) = \frac{\partial}{\partial \kappa} N(\kappa,t)\bigg|_{\kappa=1}. \tag{A15}$$

The initial conditions (3) give $\phi(0)=2$. Using the method of characteristics, we find that

$$N(\kappa,t) = \lambda \int_0^t f(\kappa,t-\tau)\phi(\tau)d\tau + 2f(\kappa,t), \tag{A16}$$

where

$$f(\kappa,t) = \frac{(\lambda + \mu)\kappa}{\lambda\kappa + (\lambda + \mu - \lambda\kappa)e^{(\lambda+\mu)t}}. \tag{A17}$$

We denote the Laplace transforms of $\phi(t)$, $N(\kappa,t)$, and $f(\kappa,t)$ by $\tilde{\phi}(s)$, $\tilde{N}(\kappa,s)$, and $\tilde{f}(\kappa,s)$, respectively, cf. Eq. (4). Taking a Laplace transform of Eq. (A16),

$$\tilde{N}(\kappa,s) = \lambda\tilde{f}(\kappa,s)\tilde{\phi}(s) + 2\tilde{f}(\kappa,s). \tag{A18}$$

By differentiating Eq. (A18) with respect to κ and setting $\kappa=1$, we find that

$$\tilde{\phi}(s) = \lambda\tilde{\phi}(s)\partial\tilde{f}/\partial\kappa|_{\kappa=1} + 2\partial\tilde{f}/\partial\kappa|_{\kappa=1}. \tag{A19}$$

Eliminating $\tilde{\phi}(s)$ from Eqs. (A18) and (A19) we obtain

$$\tilde{N}(\kappa,s) = \frac{2\tilde{f}(\kappa,s)}{1 - \lambda\partial\tilde{f}/\partial\kappa|_{\kappa=1}}. \tag{A20}$$

Taking the Laplace transform of Eq. (A17) and writing $u=e^{-(\lambda+\mu)t}$, we have

$$\tilde{f}(\kappa,s) = \int_0^{\infty} \frac{(\lambda + \mu)\kappa e^{-st}dt}{\lambda\kappa + (\lambda + \mu - \lambda\kappa)e^{(\lambda+\mu)t}} \tag{A21}$$

$$= \frac{\kappa}{\lambda + \mu} \int_0^1 \frac{u^{s/(\lambda+\mu)}du}{1 - (1-u)\lambda\kappa/(\lambda+\mu)}. \tag{A22}$$

By expanding the integral in Eq. (A22) in powers of κ and integrating term by term, we find that

$$\tilde{f}(\kappa,s) = \frac{\kappa}{s + \lambda + \mu}{}_2F_1\left(1,1;\frac{s}{\lambda+\mu} + 2;\frac{\kappa\lambda}{\lambda+\mu}\right) \tag{A23}$$

and

$$\frac{\partial\tilde{f}}{\partial\kappa}(\kappa,s) = \frac{1}{\lambda}\left({}_2F_1\left(1,1;\frac{s}{\lambda+\mu} + 1;\frac{\lambda\kappa}{\lambda+\mu}\right) - 1\right), \tag{A24}$$

where ${}_2F_1$ is the usual hypergeometric function, viz.,

$${}_2F_1(a,b;c;z) = \sum_{n=0}^{\infty} \frac{(a)_n(b)_n}{(c)_n n!}z^n, \quad (a)_n = \frac{\Gamma(n+a)}{\Gamma(a)}.$$

To determine the long-time behavior of the coordination number distribution for live nodes, we need to locate the

rightmost singularity in the complex plane for $\tilde{N}(\kappa,s)$. Candidates for singularities in Eq. (A20) arise from singularities of the numerator and from zeros of the denominator. However, the former are not singularities, as we now show. For $a>0$, $b>0$, and $|z|<1$, the singularities of $_2F_1(a,b;c;z)$ occur when $c=-m$ $(m=0,1,2,\ldots)$. From Eq. (A23), we see that $\tilde{f}(\kappa,s)$ has singularities when $s/(\lambda+\mu)=-(m+2)$ $(m=0,1,2,\ldots)$ from the $_2F_1$ function and when $s=-(\lambda+\mu)$ from the prefactor, so that all singularities are given by $s=-(m+1)(\lambda+\mu)$ $(m=0,1,2,\ldots)$. Similarly, from Eq. (A24), we see that $\partial\tilde{f}/\partial\kappa|_{\kappa=1}$ has singularities where $s=-(m+1)(\lambda+\mu)$, $m=0,1,2,\ldots$. That is, singularities of $\tilde{f}(\kappa,s)$ and $\partial\tilde{f}/\partial\kappa|_{\kappa=1}$ occur at the same values of s. As these singularities are all simple poles there is perfect cancellation and $\tilde{N}(\kappa,s)$ is not singular at these points. Thus it remains for us to locate the rightmost solution of $\lambda\partial\tilde{f}/\partial\kappa|_{\kappa=1}=1$, so we need to solve

$$_2F_1(1,1;s_p/(\lambda+\mu)+1;\lambda/(\lambda+\mu))=2. \quad (A25)$$

Given λ and μ, the value of s_p can be calculated numerically (see Fig. 3). In addition, since

$$_2F_1\left(1,1;1;\frac{1}{2}\right)=\sum_{n=0}^{\infty}2^{-n}=2,$$

we have the exact result that $s_p=0$ if $\lambda=\mu$. Also, s_p/λ may be expressed as a function of μ/λ and the asymptotic expansions given in Eqs. (35) and (36) can be established using standard results for the $_2F_1$ function.

From the inversion integral (5), as $t\rightarrow\infty$ we have

$$N(\kappa,t)\sim\operatorname*{Res}_{s=s_p}\{e^{st}\tilde{N}(\kappa,s)\}=R_1e^{s_pt}\tilde{f}(\kappa,s_p), \quad (A26)$$

where

$$R_1=\operatorname*{Res}_{s=s_p}\frac{2}{1-\lambda\partial\tilde{f}/\partial\kappa|_{\kappa=1}}. \quad (A27)$$

Let us consider now $M(\kappa,t)$, the generating function for dead nodes. Taking the Laplace transform of Eq. (A14) gives

$$\tilde{M}(\kappa,s)=\frac{\mu}{s}\kappa\frac{\partial\tilde{N}}{\partial\kappa}. \quad (A28)$$

By substituting (A20) into Eq. (A28), we see that

$$\tilde{M}(\kappa,s)=\frac{\mu}{s}\left(\frac{2}{1-\lambda\partial\tilde{f}/\partial\kappa|_{\kappa=1}}\right)\kappa\frac{\partial\tilde{f}}{\partial\kappa}(\kappa,s). \quad (A29)$$

Compare this to Eq. (33). We know already that $\partial\tilde{f}/\partial\kappa$ has the same singularity structure as $\tilde{f}(\kappa,s)$. It follows that $\tilde{M}(\kappa,s)$ has the same singularity structure as $\tilde{N}(\kappa,s)$, plus a simple pole at $s=0$. In other words, $\tilde{M}(\kappa,s)$ has singularities at $s=0$ and at $s=s_p$. We may use the inversion integral (5) to recover the asymptotic behavior of $M(\kappa,t)$ as $t\rightarrow\infty$,

$$M(\kappa,t)\sim\operatorname{Res}\{e^{st}\tilde{M}(\kappa,s)\},$$

the residue being evaluated at the rightmost pole of $\tilde{M}(\kappa,s)$. We have shown that $s_p=0$ when $\lambda=\mu$. When $\lambda>\mu$ we have $s_p>0$ and so

$$M(\kappa,t)\sim\operatorname*{Res}_{s=s_p}\{e^{st}\tilde{M}(\kappa,s)\}=\frac{\mu R_1e^{s_pt}\kappa}{s_p}\frac{\partial\tilde{f}}{\partial\kappa}(\kappa,s_p),$$

where R_1 was defined in Eq. (A27). However, when $\lambda<\mu$ we have $s_p<0$ so the pole at $s=0$ dominates,

$$M(\kappa,t)\sim\operatorname*{Res}_{s=0}\{e^{st}\tilde{M}(\kappa,s)\}=R_2\kappa\frac{\partial\tilde{f}}{\partial\kappa}(\kappa,0),$$

where $R_2=2\mu/(1-\lambda\partial\tilde{f}/\partial\kappa(1,0))$. Using a transformation formula for $_2F_1$ and Eqs. (A23) and (A25), it can be shown that $\tilde{f}(1,s_p)=(\lambda-\mu)/(\lambda s_p)$ and it follows that for $\lambda>\mu$ the limiting fraction of live nodes as $t\rightarrow\infty$ is

$$\frac{\tilde{f}(1,s_p)}{\tilde{f}(1,s_p)+(\mu/s_p)\partial\tilde{f}/\partial k(1,s_p)}=1-\mu/\lambda. \quad (A30)$$

4. Case 4: $(\lambda,\mu k)$

Taking the sum over k of Eqs. (41) and (42) gives the partial differential equations

$$\frac{\partial N}{\partial t}+\mu\kappa\frac{\partial N}{\partial\kappa}=\lambda(\kappa-1)N+\lambda\kappa\phi(t), \quad (A31)$$

$$\frac{\partial M}{\partial t}=\mu N, \quad (A32)$$

where

$$\phi(t)=N(1,t). \quad (A33)$$

The initial conditions (3) give $\phi(0)=2$. Using the method of characteristics, we find that that

$$N(\kappa,t)=\lambda\int_0^t f(\kappa,t-\tau)\phi(\tau)d\tau+2f(\kappa,t), \quad (A34)$$

where

$$f(\kappa,t)=\kappa\exp\left(-(\lambda+\mu)t+\frac{\lambda\kappa}{\mu}(1-e^{-\mu t})\right). \quad (A35)$$

Taking a Laplace transform of Eq. (A34),

$$\tilde{N}(\kappa,s)=\lambda\tilde{f}(\kappa,s)\tilde{\phi}(s)+2\tilde{f}(\kappa,s). \quad (A36)$$

Setting $\kappa=1$ gives $\tilde{\phi}(s)=2\tilde{f}(1,s)/(1-\lambda\tilde{f}(1,s))$, so

$$\tilde{N}(\kappa,s)=\frac{2\tilde{f}(\kappa,s)}{1-\lambda\tilde{f}(1,s)}. \quad (A37)$$

Taking the Laplace transform of Eq. (A35) and setting $x=e^{-\mu t}$, we have

$$\widetilde{f}(\kappa,s) = \frac{\kappa}{\mu} \int_0^1 \exp\left(\frac{\lambda\kappa}{\mu}(1-x)\right) x^{(\lambda+\mu+s)/\mu-1} dx. \quad (A38)$$

Expanding the exponential and integrating term-by-term and using Eq. (24), we deduce that

$$\widetilde{f}(\kappa,s) = \frac{1}{\lambda} \sum_{i=1}^{\infty} \frac{(\lambda\kappa/\mu)^i}{((\lambda+s)/\mu+1)_i} \quad (A39)$$

$$= \frac{\kappa}{\lambda+\mu+s} {}_1F_1\left(1; \frac{\lambda+2\mu+s}{\mu}; \frac{\lambda\kappa}{\mu}\right), \quad (A40)$$

where

$${}_1F_1(a;b;z) = \sum_{j=0}^{\infty} \frac{(a)_j z^j}{(b)_j j!}$$

is the usual confluent hypergeometric function. For $a>0$, the singularities of ${}_1F_1(a;b;z)$ are simple poles at $b=-1, -2,\ldots$, so we see that the only singularities of $\widetilde{f}(\kappa,s)$ are simple poles at $s=-\lambda-j\mu$, $j=1,2,3,\ldots$ and all poles of $\widetilde{f}(\kappa,s)$ on the numerator in Eq. (A37) are cancelled by poles on the denominator. The only singularities of $\widetilde{N}(\kappa,s)$ arise from solutions of

$$\lambda\widetilde{f}(1,s) = 1. \quad (A41)$$

If we write $\rho=\lambda/\mu$ and $\sigma(\rho)=(\lambda+\mu+s_p)/\mu$, the equation to be solved becomes

$${}_1F_1(1;\sigma(\rho)+1;\rho) = \rho^{-1}\sigma(\rho). \quad (A42)$$

Since ${}_1F_1(1;b+1;z)=(b/z)({}_1F_1(1;b;z)-1)$, we have the equivalent equation

$${}_1F_1(1;\sigma(\rho);\rho) = 2, \quad (A43)$$

which is easily solved numerically for given values of ρ. Expansions for $\sigma(\rho)$ in the limits $\rho\to 0$ and $\rho\to\infty$ can be derived and we deduce from these the asymptotic expansions given as Eqs. (46) and (47).

From the inversion integral (5), as $t\to\infty$ we have

$$N(\kappa,t) \sim \operatorname*{Res}_{s=s_p}\{e^{st}\widetilde{N}(\kappa,s)\} = R_1 e^{s_p t} \widetilde{f}(\kappa,s_p), \quad (A44)$$

where

$$R_1 = \operatorname*{Res}_{s=s_p}\{2/(1-\lambda\widetilde{f}(1,s))\}. \quad (A45)$$

Consider now $M(\kappa,t)$, the generating function for dead nodes. Taking the Laplace transform of Eq. (A32) gives

$$\widetilde{M}(\kappa,s) = \frac{\mu}{s}\kappa\frac{\partial\widetilde{N}}{\partial\kappa}. \quad (A46)$$

By substituting (A37) into Eq. (A46), we see that

$$\widetilde{M}(\kappa,s) = \frac{\mu}{s}\left(\frac{2}{1-\lambda\widetilde{f}(1,s)}\right)\kappa\frac{\partial\widetilde{f}}{\partial\kappa}(\kappa,s). \quad (A47)$$

Compare this to Eq. (A37). We know that the singularities of $\widetilde{f}(\kappa,s)$ are simple poles at $s=-\lambda-j\mu$ $(j=1,2,3,\ldots)$. Consider the singularities of $\partial\widetilde{f}/\partial\kappa$. From Eq. (A40),

$$\frac{\partial\widetilde{f}}{\partial\kappa} = \frac{\partial}{\partial\kappa}\left[{}_1F_1\left(1;\frac{\lambda+s}{\mu}+2;\frac{\lambda\kappa}{\mu}\right)\right]$$

$$= \frac{\partial}{\partial\kappa}\left\{\frac{1}{\lambda}\left[{}_1F_1\left(1;\frac{\lambda+s}{\mu}+1;\frac{\lambda\kappa}{\mu}\right)-1\right]\right\}$$

$$= \frac{1}{\lambda+\mu+s} {}_1F_1\left(2;\frac{\lambda+s}{\mu}+2;\frac{\lambda\kappa}{\mu}\right), \quad (A48)$$

so $\partial\widetilde{f}/\partial\kappa$ has simple poles at $s=-\lambda-j\mu$ $(j=1,2,3,\ldots)$. As the poles of $\widetilde{f}(1,s)$ and $\partial\widetilde{f}/\partial\kappa$ coincide, the only singularities of $\widetilde{M}(\kappa,s)$ occur at $s=s_p$, where $\widetilde{f}(1,s_p)=1/\lambda$, and at $s=0$.

We use the inversion integral (5) to recover the asymptotic behavior of $M(\kappa,t)$ as $t\to\infty$. The pole at $s=s_p$ dominates when $s_p>0$, corresponding to $\lambda>c\mu$, with $c\simeq 1.556$ (see Fig. 5), while the pole at $s=0$ dominates when $\lambda<c\mu$. We find that as $t\to\infty$,

$$M(\kappa,t) \sim \begin{cases} \dfrac{\mu}{s_p}R_1 e^{s_p t}\kappa\dfrac{\partial\widetilde{f}}{\partial\kappa}(\kappa,s_p), & \lambda>c\mu, \\[2ex] R_2\kappa\dfrac{\partial\widetilde{f}}{\partial\kappa}(\kappa,0), & \lambda<c\mu, \end{cases} \quad (A49)$$

where $R_2=2\mu/(1-\lambda\widetilde{f}(1,0))$ and R_1 was defined in Eq. (A45). We can show from Eqs. (A42), (A43), and (A48) that $\partial\widetilde{f}/\partial\kappa(1,s_p)=\mu^{-1}(1-s_p/\lambda)$. It follows that for $\lambda>c\mu$ the fraction of live nodes converges to s_p/λ as $t\to\infty$.

[1] R. Albert and A.-L. Barábasi, Rev. Mod. Phys. **74**, 47 (2002).

[2] M. Newman, SIAM Rev. **45**, 167 (2003).

[3] S. N. Dorogovtsev and J. F. F. Mendes, *Evolution of Networks* (Oxford University Press, Oxford, 2003).

[4] A.-L. Barábasi and R. Albert, Science **286**, 5439 (1999).

[5] R. Pastor-Satorras and A. Vespignani, Phys. Rev. E **63**, 066117 (2001).

[6] J. Szymánski, in *Random Graphs '87 (Poznan 1987)*, edited by

M. Karoński and A. Ruciński (Wiley, New York, 1990), pp. 313–324.

[7] J. Szymański, Ann. Discr. Math. **33**, 297 (1987).

[8] In Ref. [7], Szymański proves several results for a discrete-time tree model in which the probability of selection of a node as the next to give birth is proportional to its coordination number, including that as the tree size grows the probability that an arbitrary node has coordination number 1 converges to

2/3 and more generally, that the probability a random node has coordination number k is $4/(k(k+1)(k+2))$.

[9] D. Y. C. Chan, B. D. Hughes, A. S. Leong, and W. J. Reed, Phys. Rev. E **68**, 066124 (2003).

[10] If $\mu=0$, cases 1 and 4 reduce to the model called "Yule trees" by Chan *et al.* (Ref. [9]), while cases 2 and 3 reduce to what they call "Reed-Hughes trees," cf. W. J. Reed and B. D. Hughes, Scientiae Mathematicae Japonicae **58**, 473 (2003) [online version 8, 32 (2003)].

[11] S. N. Dorogovtsev and J. F. F. Mendes, Europhys. Lett. **52**, 33 (2000).

[12] L. A. N. Amaral, A. Scala, M. Bartélémy, and H. E. Stanley, Proc. Natl. Acad. Sci. U.S.A. **97**, 11149 (2000).

[13] C. Cooper, A. Frieze, and J. Vera, Internet Mathematics **1**, 463 (2004).

[14] D. G. Kendall, Ann. Math. Stat. **19**, 1 (1948); J. R. Stat. Soc. Ser. B. Methodol. **11**, 230 (1949).

[15] B. D. Hughes and W. J. Reed, physics/0211090 (2002).

[16] For case 1, the existence of the critical point at $\lambda=\mu$ (and certain extinction if $\lambda \leqslant \mu$) is rigorously established by classical results from the theory of linear birth and death processes (cf. Ref. [14]), though the classical theory does not explore the coordination-number distribution of the network, or other structural features.

[17] It can be shown that the mean-field threshold condition ${}_1F_1(1;\lambda/\mu+1;\lambda/\mu)=2$ is precisely the condition that the mean number of offspring per individual is 1 in an exact treatment of case 4. In this respect, the mean-field treatment returns a rigorously correct result.

[18] This standard technique for solving quasilinear partial differential equations of first order is used extensively in a similar context in Ref. [9].